

Dalton Transactions

Accepted Manuscript



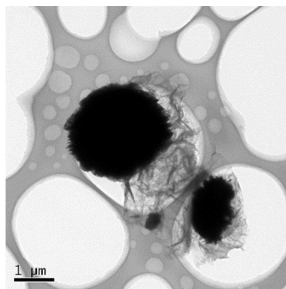
This is an *Accepted Manuscript*, which has been through the Royal Society of Chemistry peer review process and has been accepted for publication.

Accepted Manuscripts are published online shortly after acceptance, before technical editing, formatting and proof reading. Using this free service, authors can make their results available to the community, in citable form, before we publish the edited article. We will replace this *Accepted Manuscript* with the edited and formatted *Advance Article* as soon as it is available.

You can find more information about *Accepted Manuscripts* in the [Information for Authors](#).

Please note that technical editing may introduce minor changes to the text and/or graphics, which may alter content. The journal's standard [Terms & Conditions](#) and the [Ethical guidelines](#) still apply. In no event shall the Royal Society of Chemistry be held responsible for any errors or omissions in this *Accepted Manuscript* or any consequences arising from the use of any information it contains.

A novel graphene based VO₂ hydrate anode material delivers a high capacity for sodium-ion batteries.



Cite this: DOI: 10.1039/c0xx00000x

www.rsc.org/xxxxxx

ARTICLE TYPE

Stable anode performance of vanadium oxide hydrate semi-microspheres and their graphene based composite microspheres in sodium-ion batteries

Hailong Fei,^{a, b}, Zhiwei Li,^a Wenjing Feng,^a Xin Liu^a*

Received (in XXX, XXX) Xth XXXXXXXXX 20XX, Accepted Xth XXXXXXXXX 20XX
DOI: 10.1039/b000000x

A simple and versatile method for preparation of new crystalline vanadium oxide hydrate semi-microspheres is developed via a simple hydrothermal route, which are tested as a novel high-energy anode materials for sodium-ion batteries. The enhancement of electrochemical performance for vanadium oxide hydrate electrode is offered in addition of graphene. Graphene-based vanadium oxide hydrate microsphere composite shows a high discharge capacity of 336.1 Ahg⁻¹ for the second cycle between a 0.05 – 3.0 V voltage limit at a discharge current density of 10 mA g⁻¹. The reversible capacity of 303.1 Ahg⁻¹ is remained after 20 cycles.

1. Introduction

Nowadays, there is a remarkable demand for rechargeable batteries with reversible and efficient electrochemical energy storage and conversion in the field of portable electronic consumer devices, electric vehicles, and large-scale electricity storage in smart and intelligent grids [1]. Sodium-ion battery is one of the promising rechargeable batteries for its huge abundant and low cost sodium resources [2]. However, it is difficult to find a kind of anode materials that can insert and remove sodium ion reversibility just like that commercial graphite does in the lithium-ion battery, which restricts the future application of sodium-ion batteries. The discovery of commercial and applicable anode materials for sodium-ion batteries is a matter of great urgency. The current concerns are leading to an increasing interest in low cost, high safety anode materials for sodium-ion batteries with a long cycle life and high energy-density. Now researchers in growing numbers are coming to pay attention to the electrochemical properties of various anode materials, for example, carbon-graphene composite [3], carbon nanosheets [4], Sn [5] and Sb [6], Sn-P composites [7], titanate [8] amorphous phosphorus-carbon composite [9, 10], sulfide [11], organic sodium-ion batteries [12] and so on.

Vanadium oxides and bronzes offer the advantages of being cheap, easy to synthesize, plenty of the earth and high-energy density. Therefore, they have attracted many interests in energy conversion and storage [13]. A few interests were attracted to study vanadium oxide [14-18], sodium vanadate nanostructures [19, 20], hollow VOOH microspheres [21] and ammonium vanadium bronze as cathode materials for sodium-ion batteries [22-24]. Few attention was attracted to vanadium oxide anode materials for sodium-ion batteries [25].

Herein, we report the synthesis of new crystalline vanadium oxide hydrate semi-microspheres via a simple hydrothermal

method requiring low cost manufacturing and ultra-low power consumption. When they were used as anode materials for sodium-ion batteries, graphene based vanadium oxide hydrate microspheres showed better cycling stability and higher discharge capacity.

2. Experimental

Vanadium oxide hydrate semi-microspheres were prepared according to the following procedure. 1.44 g oxalic acid and 0.4 g ammonium metavanadate (NH₄VO₃) were dissolved in 30 ml deionized water under stirring at room temperature for 2 hours. After that, the mixture was transferred to a 50-ml Teflon-lined stainless autoclave, sealed, kept at 200 °C for 24 hours, cooled to room temperature, washed with deionized water and dried at 70 °C for 12 hours. Under the same procedure, graphene based composites were prepared with 1.44 g oxalic acid, 0.4 g ammonium metavanadate (NH₄VO₃) and 3 mg graphene.

The morphological characteristics of the as-synthesized materials were observed with a Hitachi S-4800 field emission scanning electron microscope (SEM). Transmission electron microscopy (TEM) was carried out on a FEI Tecnai G20 electron microscopy instrument. X-ray diffraction (XRD) patterns were recorded on a diffractometer (Co K α , PANalytical, and X'Pert). XPS measurements were performed with a Kratos Axis Ultra DLD spectrometer employing a monochromated Al-K α X-ray source (h ν = 1486.6 eV). A pass energy of 160 eV was used for recording the survey spectrum, while 40 eV pass energy was used for high-resolution measurements. The element analyses were performed with a Vanio-EL analyzer Solaar S2 and a Vario EL elemental analyzer from German Elementar Analysen Systeme GmbH. Thermal analysis measurements were performed using a Rigaku TG-DT Analyzer. Raman spectrum was recorded at room temperature using a Micro-Raman spectrometer from English renishawn. An Nd: YAG laser (532 nm) was used as the

excitation source. A Land CT2001A battery tester was used to measure the electrode activities at room temperature.

The vanadium oxide hydrate semi-microspheres and their composites based on graphene were tested as anode materials for sodium-ion batteries. The composite of negative electrode material was consisted of the active material, a conductive material (super-pure carbon) and binder polyvinylidene difluoride (PVDF) in a weight ratio of 7/2/1. The Na metal was used as the counter electrode. The electrolyte was 1 M NaClO₄ dissolved in propylene carbonate (PC) solvent with an addition of 5% weight fluoroethylene carbonate (FEC). The cells were charged and discharged between a 0.05 - 3.0 V voltage limit at a current density of 10 mA g⁻¹.

3. Results and discussion

Vanadium oxide hydrate and its composite based on graphene were prepared by a facile hydrothermal method, as described in the experimental section. X-ray diffraction was performed to identify the crystalline structure of the as-synthesized sample and graphene based composite in Fig. 1a and b, respectively. For graphene based composite, extra small peaks appear at 19.25°, 21.24°, 22.52°, 32.57°, 38.74°, 53.54° and 56.72°, which implies the presence of un-pure crystalline phase. The two samples cannot be ascribed to the known compounds in the XRD database.

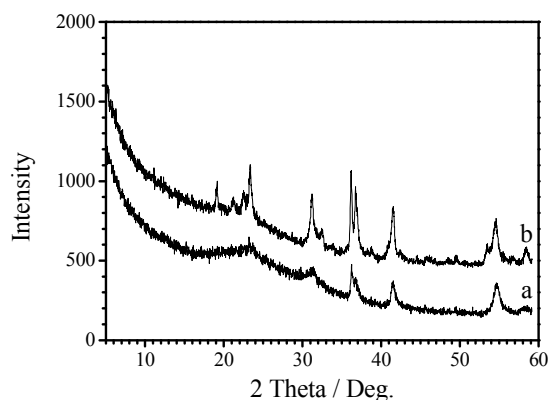


Fig. 1 Wide-angle powder XRD patterns of (a) the as-synthesized sample and (b) graphene based composite.

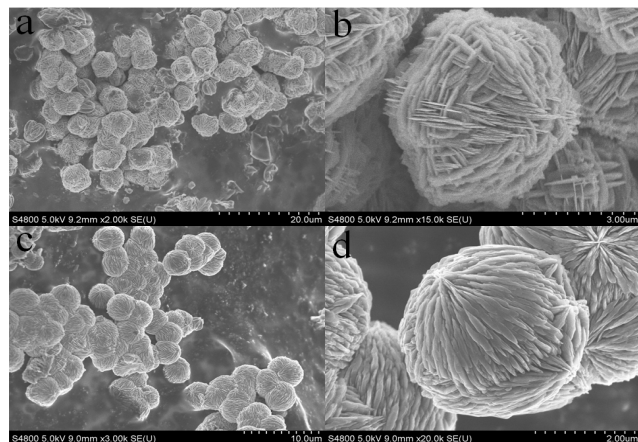


Fig. 2 SEM images of the as-synthesized materials (a, b) and graphene based composite (c, d).

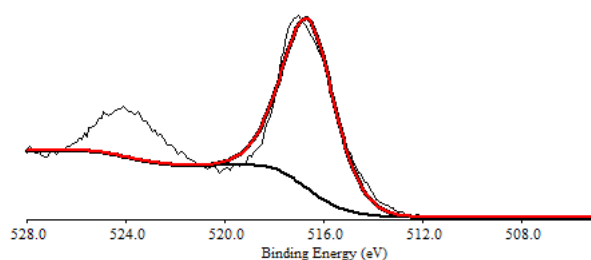


Fig. 3 V2p high-resolution XPS spectrum of the as-synthesized sample.

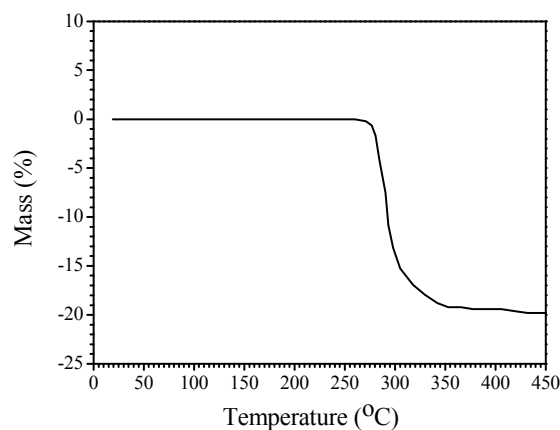


Fig. 4 TG curve of the as-synthesized sample.

SEM observations show that the as-synthesized sample is semi-microspheres, as shown in Fig. 2a. The magnified SEM image confirms that semi-microsphere-like particles are consisted of superimposed platelets in Fig. 2b. Under our experimental condition for the presence of superfluous oxalic acid, it is very difficult to get vanadium precursor precipitate except blue solution for a short period of reaction time. A small amount of precipitate with a morphology of microspheres was obtained at 200 °C for 24 h. Therefore, we did not perform time-dependent experiments to research the formation process of microspheres. According to our understanding and experiences, at initial stage of reaction, NH₄VO₃ was reduced to VO²⁺ by oxalic acid and the excess oxalic acid would react with VO²⁺ to form V(IV)O(C₂O₄)₂²⁻[26]. During hydrothermal treatment at 200 °C, primary crystallites were slowly formed and fast organized to microspheres for minimize surface free energy. In the further process of crystal growing or phase converting, the nanoflakes may form on the surface and they would spontaneous assemble to from regular arrays. As some graphene was added, the adjacent microspheres were obtained in Fig. 2c. The magnified SEM image shows that the microspheres are consisted of superimposed rods as a top in Fig. 2d.

X-ray photoelectron spectroscopy (XPS) was performed to identify the element covalence of V. The V2p high-resolution XPS spectrum of the as-synthesized sample shows a wide peak at 516.6 eV, corresponding to V (IV) in Fig. 3 [24]. Element analysis (EA) shows that there is no N element in the as-

synthesized sample. TG curve (Fig. 4) shows that there is a weight loss of 19.4% from 250 to 400 °C, due to the release of H₂O. Based on the above analysis, the formula of the as-synthesized sample can be expressed as VO₂•1.65H₂O.

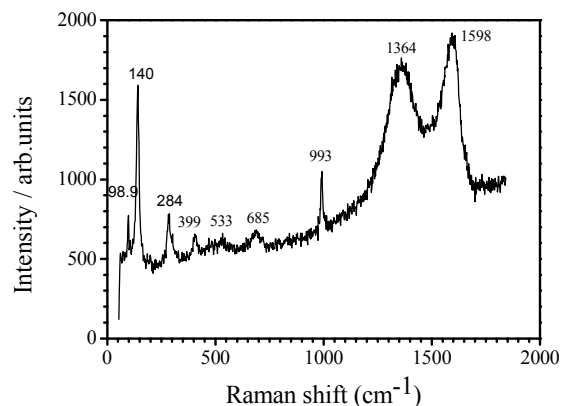


Fig. 5 Raman spectrum of graphene based composite.

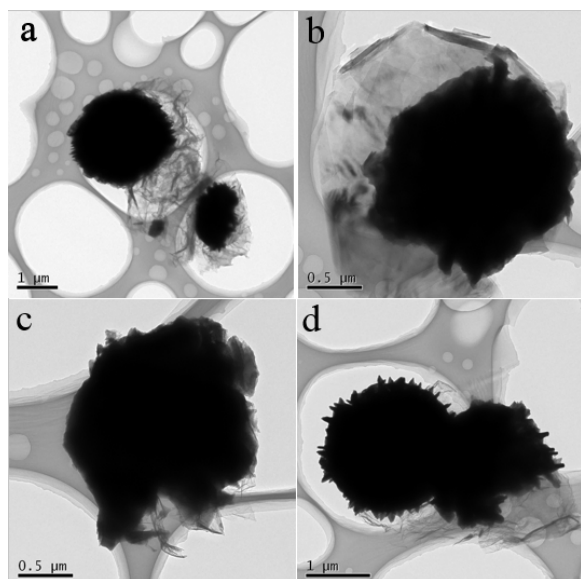


Fig. 6 TEM images of graphene based composite.

Raman spectrum of graphene based vanadium oxide hydrate composite exhibits a series of bands at 142, 194, 281, 405, 520, 689, 990, 1351 and 1589 cm⁻¹ same to those of V₂O₅ in Fig. 5. The peak at 990 cm⁻¹ is characteristic of the V=O bond. Because there is no Raman peaks for VO₂•1.65H₂O semi-microspheres. The above peaks can be ascribed to the un-pure phase in the graphene based materials. The band at 1351 cm⁻¹ is called the D band [27], which is a disorder induced band [28]. The band at 1589 cm⁻¹ is ascribed to the G band due to the symmetry of the hexagonal lattice, which allows only one first order Raman band for graphene [28]. Therefore, Raman spectrum shows that there are at least two kinds of carbon (disorder carbon and graphene) in the graphene based composite. Element analysis (EA) was used to analyze the content of graphene. There is weight 5.6% graphene. Transmission electron microscopy (TEM) was further performed to study graphene based composite. Black sphere-like particles surrounded by thick layers of thin graphene sheets were observed and displayed in Fig. 6a. Fig. 6b shows that an image of

graphene block can be linked to the surface of microspheres. Fig. 6c and d show that a little graphene is dispersed to the fringe of microspheres. So graphene is on the surface of vanadium oxide hydrate with a different amount.

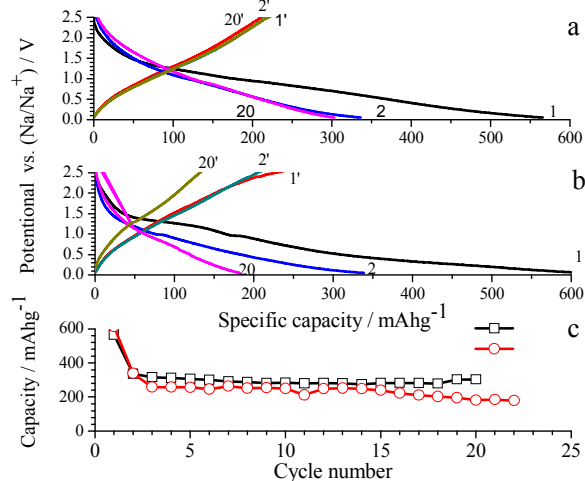


Fig. 7 The 1st, 2nd and 20th charge-discharge profiles of (a) graphene based composite, (b) VO₂•1.65H₂O semi-microspheres and (c) The cycling performance of vanadium oxide hydrate semi-microspheres (○) and graphene based composite (□).

The electrochemical performance of VO₂•1.65H₂O and its graphene composite were evaluated. Fig. 7a and b show the 1st, 2nd and 20th charge-discharge profiles of graphene based composite and VO₂•1.65H₂O semi-microspheres at a current density of 10 mA g⁻¹, respectively. It can be observed that both have similar charge-discharge profiles in shape. But graphene based composite shows better charge properties for the superposition of the charge curves. Fig. 7c shows their cycling performance. The graphene based composite electrode shows an enhanced cycling performance compared to VO₂•1.65H₂O semi-microspheres. The graphene based composite electrode delivers a second discharge capacity of 336.1 mA h g⁻¹. A reversible capacity of 303.1 mA h g⁻¹ is remained after 20 cycles. As for VO₂•1.65H₂O semi-microspheres, the second discharge capacity is 338.8 mA h g⁻¹. A reversible capacity of 181.9 mA h g⁻¹ is remained after 20 cycles. The second discharge capacity is 338.8 and 336.5 mA h g⁻¹ for VO₂•1.65H₂O semi-microspheres and graphene based microspheres, which corresponds to 1.42 and 1.41 Na⁺ inserting to one VO₂•1.65H₂O molecule. The possible electrochemical process is as following: VO₂•1.65H₂O + xNa⁺ + xe⁻ ↔ Na_xVO₂•1.65H₂O (0 < x ≤ 1.42). The capacity decay during cycling is ascribed to the bad conductivity of electrode materials, the irreversible sodium ion inserting and deintercalation and slow transfer rate of sodium ion for large ion radius. Further work will concentrate on overcoming those problems by the modification of electrode materials' crystalline structure via intercalation of Na⁺ and improving the electrolyte, glass fiber film, binder and conductive materials. For example, Super P, and sodium carboxymethyl cellulose / poly (acrylic acid) (1:1) would be used to take the place of super-pure carbon and PVDF, respectively. Decreasing particle size is also in consideration for the improvement of electrochemical performance. It would be apt to prepare larger particles at sub-micrometer / micrometer scale via hydrothermal route. Sol-gel, solvo-thermal and solid phase synthesis may be the facile methods to prepare nano-size particles. Small particles, such as nanoparticles, would have high surface area and reduce the ionic and electronic diffusion distance to promote the penetration of sodium ion and electrons to

electrode materials easier [29]. Therefore, the notable improvement of electrode performance would be gained around.

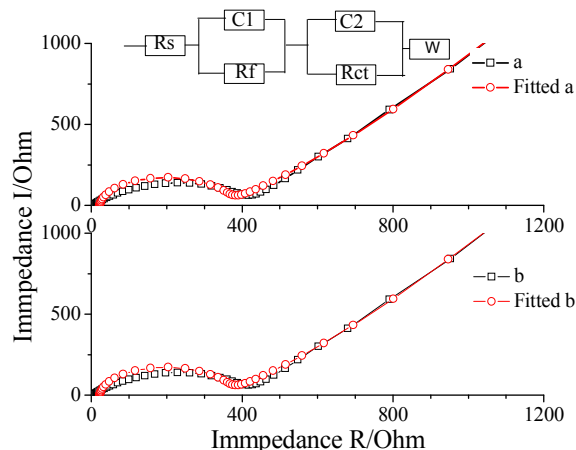


Fig. 8 Nyquist-diagram of graphene based composite (a) and $\text{VO}_2 \cdot 1.65\text{H}_2\text{O}$ (b) after discharging and charging for 1 cycle (inset is the fitting impedance circuit model).

The electrochemical impedance measurements were performed to elucidate the difference in electrochemical properties of graphene based composite and $\text{VO}_2 \cdot 1.65\text{H}_2\text{O}$ in Fig. 8. It can be found that both have the same fitting impedance circuit model and similar total impedance. The equivalent electrical circuit consists of an active electrolyte resistance R_s in series with the parallel combination of the double-layer capacitance C_1 , C_2 and an impedance of a faradaic reaction. In this model, the impedance of a faradaic reaction consists of an active charge transfer resistance R_{ct} and a specific electrochemical element of diffusion W called Warburg element.

4. Conclusions

$\text{VO}_2 \cdot 1.65\text{H}_2\text{O}$ semi-microspheres and its composites based on graphene microspheres were prepared with cheap reagents at a large scale via a facile template-free method. The enhancement of electrochemical performance for $\text{VO}_2 \cdot 1.65\text{H}_2\text{O}$ semi-microspheres is offered in addition of graphene. This facile method is significant to fabricate other novel crystalline sodium-ion battery anode materials with high discharge capacity.

Acknowledgments

The project was supported by the National Natural Science Foundation of China (Grant No. 51204058), the fund (JA12037) from the Fujian Education Department, the open project in Key Lab Adv. Energy Mat. Chem. (Nankai University) (KLAEMC-OP201201) and the State Scholarship Fund from the China Scholarship Council (CSC).

Notes and references

^a College of Chemistry, Fuzhou University, 523 Industry Road, Fuzhou 350002, P.R. China. Tel (Fax): +86 591 87760172; E-mail: feilin09053@gmail.com

^b Key Laboratory of Advanced Energy Materials Chemistry (Ministry of Education), Collaborative Innovation Center of Chemical Science and Engineering (Tianjin), College of Chemistry, Nankai University, Tianjin 300071, China. E-mail: fimer99@163.com

1 F. Y. Cheng, J. Liang, Z. L. Tao and J. Chen, *Adv. Mater.*, 2011, **23**, 1695.

- 2 H. L. Pan, Y. S. Hu and L. Q. Chen, *Energy Environ. Sci.*, 2013, **6**, 2338.
- 3 Y. Yan, Y. X. Yin, Y. G. Guo, and L. J. Wan, *Adv. Energy Mater.* 2014, **4**, 1301584.
- 4 J. Ding, H. L. Wang, Z. Li, A. Kohandehghan, K. Cui, Z. W. Xu, B. Zahiri, X. H. Tan, E. M. Lotfabad, B. C. Olsen, and D. Mitlin, *ACS nano*, 2014, **12**, 11004.
- 5 H. L. Zhu, Z. Jia, Y. C. Chen, N. Weadock, J. Y. Wan, O. Vaaland, X. G. Han, T. Li, and L. B. Hu, *Nano Lett.* 2013, **13**, 3093.
- 6 J. F. Qian, Y. Chen, L. Wu, Y. L. Cao, X. P. Ai and H. X. Yang, *Chem. Commun.*, 2012, **48**, 7070.
- 7 W. J. Li, S. L. Chou, J. Z. Wang, J. H. Kim, H. K. Liu, and S. X. Dou, *Adv. Mater.*, 2014, **26**, 4037.
- 8 H. J. Yu, Y. Ren, D. D. Xiao, S. H. Guo, Y. B. Zhu, Y. M. Qian, L. Gu, and H. S. Zhou, *Angew. Chem. Int. Ed.*, 2014, **53**, 8963.
- 9 J. F. Qian, X. Y. Wu, Y. L. Cao, X. P. Ai and H. X. Yang, *Angew. Chem. Int. Ed.*, 2013, **52**, 4633.
- 10 W. J. Li, S. L. Chou, J. Z. Wang, H. K. Liu and S. X. Dou, *Nano Lett.* 2013, **13**, 5480.
- 11 Z. Hu, L. X. Wang, K. Zhang, J. B. Wang, F. Y. Cheng, Z. L. Tao, and J. Chen, *Angew. Chem. Int. Ed.*, 2014, DOI:10.1002/ange.201407898.
- 12 S. W. Wang, L. J. Wang, Z. Q. Zhu, Z. Hu, Q. Zhao and J. Chen, *Angew. Chem. Int. Ed.*, 2014, **126**, 6002.
- 13 F. Y. Cheng and J. Chen, *J. Mater. Chem.*, 2011, **21**, 9841.
- 14 D. Hamani, M. Ati, J. M. Tarascon and P. Rozier, *Electrochem. Commun.* 2011, **13**, 938.
- 15 M. Z. A. Munshi, A. Gilmour, W. H. Smyrl and B. B. Owens, *J. Electrochem. Soc.*, 1989, **136**, 1847.
- 16 H. L. Fei, Y. S. Lin, and M. D. Wei, *J. Colloid Interf. Sci.* 2014, **425**, 1.
- 17 S. Tepavcevic, H. Xiong, V. R. Stamenkovic, X. B. Zuo, M. Balasubramanian, V. B. Prakapenka and C. S. Johnson, *ACS Nano*, 2012, **6**, 530.
- 18 D. W. Su and G. X. Wang, *ACS Nano*, 2013, **7**, 11218.
- 19 H. M. Liu, H. S. Zhou, L. P. Chen, Z. F. Tang and W. S. Yang, *J. Power Sources*, 2011, **196**, 814.
- 20 H. N. He, G. H. Jin, H. Y. Wang, X. B. Huang, Z. H. Chen, D. Sun and Y. G. Tang, *J. Mater. Chem. A*, 2014, **2**, 3563.
- 21 J. Shao, Y. L. Ding, X. Y. Li, Z. M. Wan, C. Y. Wu, J. P. Yang, Q. T. Qu and H. H. Zheng, *J. Mater. Chem. A*, 2013, **1**, 12404.
- 22 H. L. Fei, X. M. Wu, H. Li and M. D. Wei, *J. Colloid Interf. Sci.*, 2014, **415**, 85.
- 23 H. L. Fei, X. Liu, H. Li and M. D. Wei, *J. Colloid Interf. Sci.*, 2014, **418**, 273.
- 24 H. L. Fei, H. Li, Z. W. Li, W. J. Feng, X. Liu and M. D. Wei, *Dalton Trans.*, 2014, DOI: 10.1039/c4dt02002b.
- 25 C. Deng, S. Zhang, Z. Dong, and Y. Shang, *Nano Energy*, 2014, **4**, 49.
- 26 H.L. Fei, H.J. Zhou, J.G. Wang, P.C. Sun, D.T. Ding, and T.H. Chen, *Solid State Sci.*, 2008, **10**, 1276.
- 27 R. P. Vidano, D. B. Fischbach, L. J. Willis, and T. M. Loehr, *Solid State Commun.*, 1981, **39**, 341.
- 28 V. Zólyomi, J. Koltai, and J. Kürti, *Phys. Status Solidi B*, 2011, **248**, 2435.
- 29 W. Wang, B. Jiang, L.W. Hu, Z.S. Lin, J.G. Hou, and S.Q. Jiao, *J. Power Sources*, 2014, **250**, 181.